JOURNAL OF OPTOELECTRONICS AND ADVANCED MATERIALS Vol. 12, No. 12, December 2010, p. 2343 - 2354

Characteristics and applications of tilted fiber Bragg gratings

YONG ZHAO*, QI WANG, HE HUANG
Northeastern University, School of Information Science and Engineering, Shenyang 110819, China

In this paper, the fabrication methods and spectral characteristics of tilted fiber Bragg gratings(TFBG) are described. The principles of coupling to cladding modes and radiation modes are mainly investigated. The polarization dependent characteristics of TFBG are also emphasized. According to these optical properties introduced above, examples are given to illustrate the various applications of TFBG in the investigation of sensors, interrogators, gain flattened fiber amplifiers, optical fiber filters, polarimeters, polarization-dependent loss equalizers and so on. The potential feasibility of cooperating TFBG with other sensing mechanism(such as SPR) is also discussed.

(Received November 22, 2010; accepted November 29, 2010)

Keywords: Tilted fiber Bragg gratings, Mode coupling, Polarization, Optical fiber sensor, Optical fiber devices

1. Introduction

Fiber optic gratings are developing fast in recent years as a novel passive fiber optic device charactering small volume, high sensitivity and easy to wavelength division multiplex. It is widely used in fiber optic sensors and fiber optic communications. Titled fiber Bragg gratings are also called slanted gratings or blazed gratings which is a special kind of short-term fiber optic gratings. Like normal fiber Bragg gratings, titled fiber Bragg gratings have periodical index variation in axial direction. The boundary surface of the varied index is not vertical with respect to the fiber axis but has a certain angle, which gives titled fiber Bragg gratings some particular characteristics other than normal fiber Bragg gratings. One feature of tilted fiber Bragg gratings is that they can couple guided-modes with copropagating modes or counterproagating modes in specific wavelengths. Because of this characteristic, tilted fiber Bragg gratings can be used as gain flattened erbium fiber amplifiers[1], optical spectrum analyzers[2,3], modal power distribution measurers[4], add-drop filters[5, 6] and etc. Another feature of tilted fiber Bragg gratings is that they are sensitive to the surrounding refractive index outside the gratings, due to which they can be functioned as refractometers[7-9] and concentration meters[10, 11]. Tilted fiber Bragg gratings which have large tilt angles are also show good sensitivity to the polarization state of the incident light. Therefore, they can be served as polarimeters[12-14], twist sensors[15] and polarization-dependent loss equalizers[16].

2. Fabrication methods

There are several methods to fabricate tilted fiber Bragg gratings. Among them, the phase mask method[12, 17, 18] and the interferometric method[8, 19] are mostly used. Fig.1 shows the schematic of the setup to fabricate tilted fiber Bragg gratings using phase mask. There are two ways to space the fiber when using phase mask method. One way is, as shown in Fig.1(a), that the fiber is placed in front of the phase mask as shown. There is a tilt angle θ between the phase mask plane and the fiber. The ultraviolet beam is perpendicular to the phase mask plane. The tilt angle of the TFBG fabricated is θ. This way of placing the fiber can only be used to fabricate small tilt angle TFBGs[18]. The other way is, as shown in Fig.1(b), that the fiber is oriented at an azimuthal tilt angle φ with respect to the fringe pattern and the phase mask plane is oriented at an elevation angle ϕ with respect to the plane normal to the collimated excimer ultraviolet beam. By varying the two angles φ and ϕ a tilt angle θ can be imprinted in the grating, which can be denoted by

$$\theta_B = \cos^{-1}\left(\left(\tan^2\phi' + \tan^2\left(\frac{\pi}{2} - \tan^{-1}\left(\frac{n}{(2-n)\tan\theta}\right)\right)+1\right)^{-\frac{1}{2}}\right) \quad (1)$$

where n is the refractive index of the fiber at the wavelength of the excimer ultraviolet light, $n\sin\phi' = \sin\phi$, from Snell's law. [16]

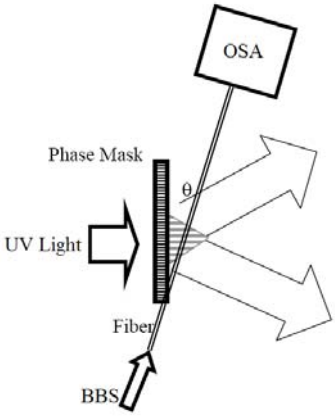

(a)

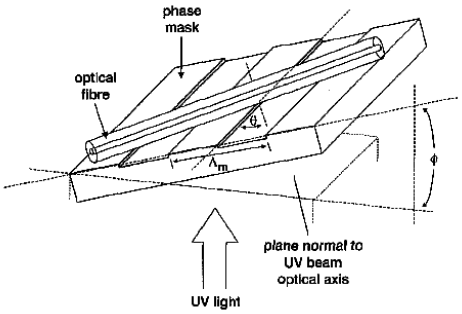

(b)

Fig.1 Schematic of the setup to fabricate tilted fiber Bragg gratings using phase mask.

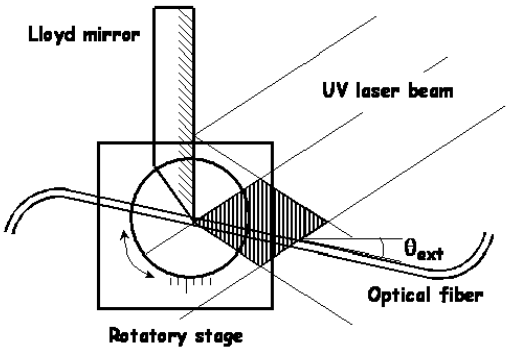

Fig. 2. Interferometer setup for the photo-writing of TFBGs.

Another method to fabricate tilted fiber Bragg gratings is shown in Fig. *2*. The Lloyd mirror interferometer is used in the fabrication. The fiber is fixed on a rotatory stage to adjust the tilt angle. The angle between the fiber axis and the normal to the fringe pattern, the external tilt angle, is denoted θ_{ext}. The ultraviolet beam intersection angle in air is denoted as $2\alpha_{ext}$, the relation between θ_{ext} and θ is[17]

$$\theta_{ext} = \frac{1}{2}\sin^{-1}\left(n_{clad}\sin\left(\frac{n_{eff}}{n_{clad}}\cdot\frac{\lambda_{UV}}{\lambda_{Bragg}\cos\theta}+\theta\right)\right) - \frac{1}{2}\sin^{-1}\left(n_{clad}\sin\left(\frac{n_{eff}}{n_{clad}}\cdot\frac{\lambda_{UV}}{\lambda_{Bragg}\cos\theta}-\theta\right)\right) \quad (2)$$

where n_{clad} is the refractive index of fiber cladding, and n_{eff} is the effective refractive index of the bound mode. λ_{UV} is the wavelength of excimer ultraviolet light, and λ_{Bragg} is the design Bragg wavelength of grating. In both methods, the transmission spectrum is being monitored in real time during the fabrication.

3. Structures and characteristics

3.1 Structures

TFBGs belong to the short-period grating family but their index modulation patterns are tilted by an angle ξ with respect to the fiber axis. The structure of TFBG is shown in Fig.3. In a single mode fiber, the tilted angle of the grating planes enhances the coupling of the light from the forward-propagating core mode to backward propagating cladding modes and reduces the coupling to the backward core mode. The Bragg reflection and cladding mode resonance wavelength λ_{Bragg} and $\lambda_{\text{coupling},i}$ of TFBG are determined by the phase-matching condition and can be expressed as follows

$$\lambda_{Bragg} = \frac{2n_{co,eff}\Lambda}{\cos\xi} \quad (1)$$

$$\lambda_{coupling,i} = \frac{\left(n_{co,eff} + n_{clading,i,eff}\right)\Lambda}{\cos\xi} \quad (2)$$

where ξ is the tilt angle, $n_{co,eff}$ and $n_{clading,i,eff}$ are the effective refractive index of the core mode and the *i*th cladding mode, respectively. Λ corresponds to the nominal grating period and can be described as $\Lambda = \Lambda_g \cdot \cos\xi$. In this relationship, Λ_g denotes the grating period along the axis of the fiber.

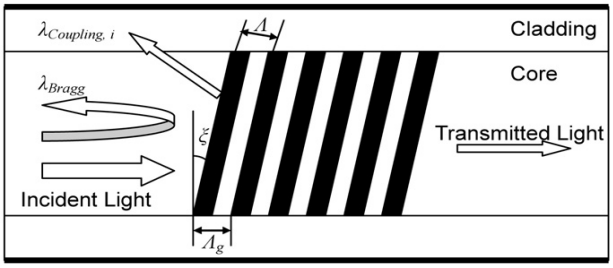

Fig. 3. Diagram of the core of a tilted fiber Bragg gratings.

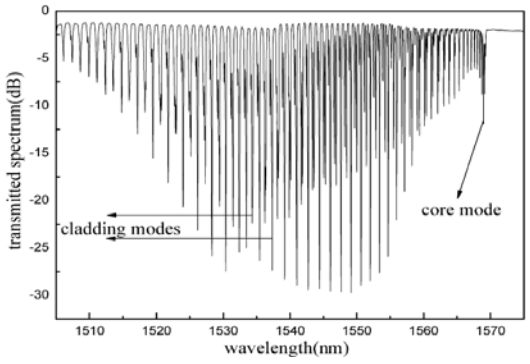

Fig.4 Transmission spectrum of a TFBG.

These two kinds of couple in the TFBG result in the appearance of the core mode and a lot of cladding-mode resonances in the transmission spectrum of TFBG, which is shown in Fig.4. The contra-propagating cladding modes attenuate rapidly and are therefore not observable in reflective spectrum but are observed as numerous resonances in the transmission spectrum of the TFBG.

3.2 Reducing of Fringe Visibility

The main effect of grating tilted in a single-mode fiber Bragg grating is that it effectively reduces fringe visibility[20]. As an example, Fig. 5 shows a plot of the normalized effective fringe visibility as a function of tilt angle θ for the LP01 mode in a fiber with a cladding index of 1.44, a core-cladding $\Delta = 0.0055$, a core radius of $a = 2.625\ \mu m$, and at a wavelength of 1550 nm.

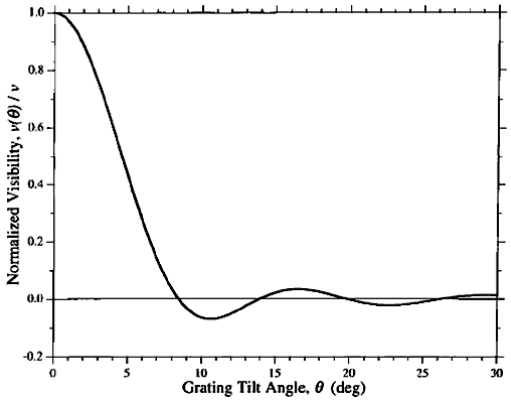

Fig. 5. Plot of the normalized effective fringe visibility associated with single-mode Bragg reflection in a tilted grating in the core of a fiber with parameters described in the text.

3.3 Polarization Dependence of TFBG

As illustrated in the previous discussion ,tilted or blazed fiber Bragg gratings (TFBGs) can couple light from guided modes into radiation modes. The light source polarization can affect the efficiency of coupling because tilted fiber gratings are asymmetric gratings. In a small tilted angle gratings ($\theta < 15^{\circ}$), the effect of source polarization is insignificant[17]. However, TFBGs at large tilted angles are highly polarization sensitive [21, 17]. For an FBG tilted at 45° with respect to the fiber axis, there is a difference of two orders of magnitude between radiation mode coupling for s-polarized (in the plane of the tilted index modulation) and p-polarized light [22,23].

These characteristic allows TFBG in the investigation and fabrication of all fiber polarimeter, polarization-dependent loss equalizer, in-fiber twist sensors and so on.

4. Applications

As we have known that TFBG can couple light from guided modes into radiation modes or cladding modes, and the efficiency of coupling by a TFBG at large tilt angles is sensitive to light polarization state, various sensors and devices based on these characteristics have been proposed or developed for broad applications .

4.1 Sensors and measurement applications

4.1.1 Chemical Sensors

Geraled Meltz et al. (1993) applied tilted fiber Bragg gratings in a chemical sensor[24]. It uses a grating radiation coupler to excite fluorescent in a short length of an absorbing jacket which contains the analyte and a suitable fluorophore. Light is collected from the emitted fluorescent layer by the refractive index perturbations in the core which form very weakly reflecting dielectric mirrors.

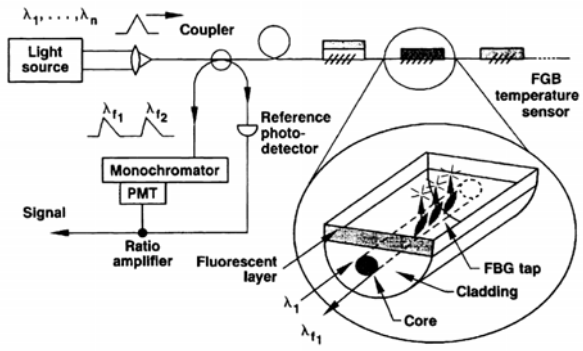

Fig. 6. Schematic of a multipoint tilted fiber Bragg grating chemical sensor system[24].

Fig. 6 shows the schematic of a multipoint tilted fiber Bragg grating chemical sensor system. The tilted grating can be formed in a fiber which has a D-shaped cladding by exposing the core to a two-beam interference pattern

ultraviolet. The fluorescent molecules can be incorporated into the fiber cladding or into a permeable layer that is deposited at the cladding interface. The material being analyzed is illuminated by the light which is coupled out of the fiber core by the grating. The grating acts as an array of dielectric thin film weakly reflecting mirrors, which redirect a fraction of the photoinduced luminescence into the acceptance cone of the fiber core. The coupling sensitivity will be larger if a multimode fiber grating designed to couple light at shallow Bragg angles is used. Overall transfer efficiencies of 10^{-4} to 10^{-2} are expected by using highly photosensitive fibers.

4.1.2 Interrogator of FBG sensors

As we know, chirped TBFG can couple the light at different wavelengths out of the fiber core into radiation mode along the grating in different directions. If the grating is linear chirped, the radiation light will be linear distributed. This feature can be used to interrogating FBG sensors[25-29]. The radiation light can be measured by either photodetector linear array[25, 26, 29] (as shown in Fig.7) or linear array CCD[27, 28] (as shown in Fig.8).

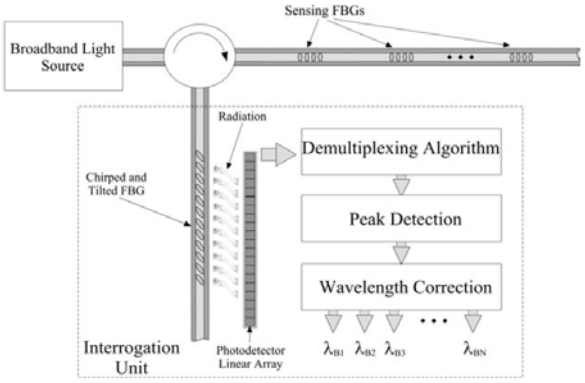

Fig. 8 Interrogation of FBG sensors using TFBG and photodetector linear array[26].

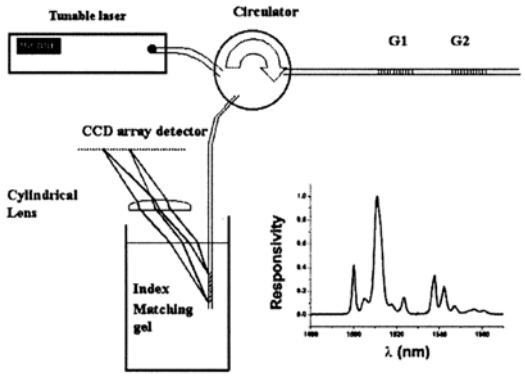

Fig. 9. Interrogation of FBG sensors using TFBG and CCD[27].

Note that normal CCD is not sensitive to the infrared radiation. CCD array used in these experiments were coated with Y2O2S: Er, Yb to sensitize the array to the light in infrared wavelength. In general, although the response of this coated CCD is highly nonlinear, this device offers high resolution and a good level of system stability.

This kind of FBG sensors interrogation system based on the detection of radiation light out coupled from TFBG will become invaluable to smart structure and other field applications due to its extremely low cost, compact structure, large dynamic range and high resolution.

4.1.3 Refractometers

Tilted fiber Bragg gratings are sensitive to the external refractive index. Hence, TFBG can constitute accurate refractometers [7, 9, 30] and they can advantageously be used in a lot of chemical and biochemical applications.

The cladding modes are guided by the cladding boundary, and their effective index depends on the refractive index of the outer medium. By monitoring the changes of the cladding modes, an accurate measure of the external refractive index can be obtained.

The schematic of a TFBG refractometer, which is able to measure the external refractive index with single-end access, is shown in Fig.10[9]. The fiber was cleaved off after the grating and the end surface was coated with Au. The transmitted light can be reflected back at the end surface.

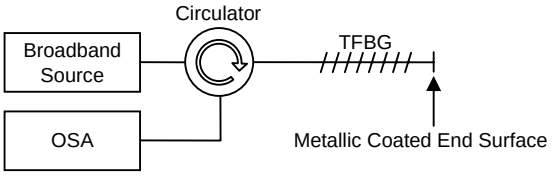

Fig.10. Schematic of the TFBG refractometer (OSA: optical spectrum analyzer)

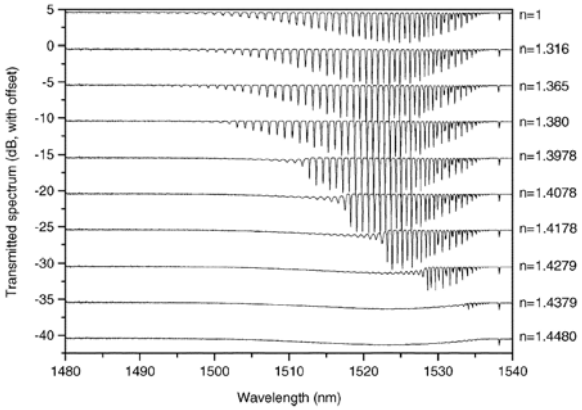

Fig.11. Evolution of the 4°TFBG transmitted spectrum in different refractive index media[7].

Fig.11 shows the dependence between surrounding refractive index and transmitted spectrum of TFBG, from which we can see that the refractive indices can not be explicitly told from the transmitted spectrum. C. Caucheteur et al. (2005) have presented a demodulation technique for tilted fiber Bragg grating refractometer[7]. The interrogation technique is based on the monitoring of the upper and lower envelopes of the cladding modes spectrum. By using this technique, C. Caucheteur successfully measured surrounding refractive index measurement in the range 1~1.45[7].

Another interrogation technique was presented by Chun-Fan Chan et al. (2007). The temperature dependence of the cladding mode wavelength shifts relative to Bragg wavelength is very small. Thus, by monitoring the shifts of the cladding modes relative to the Bragg resonance, an accurate measure of the external refractive index can be obtained. This method allows the measurement of the refractive index of the medium surrounding the fiber for values between 1.25 and 1.44[9].

In comparison with long-period gratings (LPGs), TFBGs are more compact and less sensitive to bending. With proper interrogation method, tilted TFBGs can measure both the surrounding refractive index and temperature simultaneously.

4.1.4 In-fiber Twist Sensors

As TFBGs have a strong polarization dependent coupling behavior, they can be utilized as in-fiber twist sensor. By making the tilted angle θ >45°, TFBGs are capable of coupling light from core mode to forward-propagating cladding modes[31]. Such gratings have exhibited pronounced polarization mode split characteristics[15]. Polarization state changes together with fiber twist. By measuring the polarization state, the twist angle can be obtained. Therefore, it is possible to interrogate a TFBG in-fiber twist sensor using low-cost intensity demodulation technique.

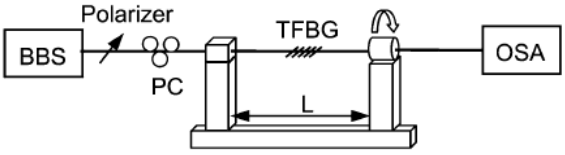

Fig.12 Schematic of TFBG based twist sensor. (BBS: broadband light source; PC: polarization controller; OSA: optical spectrum analyzer.)[15].

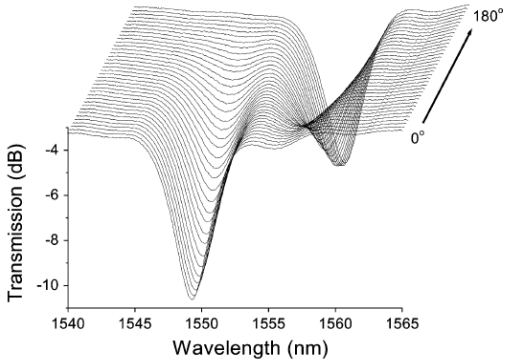

Fig.13. Spectra evolution of TFBG twist sensor under twist in clockwise direction from 0° to 180°.

The schematic of the experiment to implement the optical twist sensor is illustrated in Fig. 12. A fiber with a 10-mm-long 81° TFBG positioned in the middle was fixed by a clamp on one side and a fiber rotator on the other. Before the fiber was twisted, polarization controller was inserted to adjust the pre-polarization at a state that only the peak on the shorter wavelength side was fully excited. As the fiber is twisted from 0° to 180°, the strength of that peak decreases, but the peak on the longer wavelength side grows. When the fiber is rotated by 180°, the peak on the shorter wavelength completely vanishes and the peak on the longer wavelength reaches its maximum strength, as shown in Fig.13.

4.1.5 Bending Sensors

A new type fiber bending sensor based on a tilted fiber Bragg grating (TFBG) interacting with a multimode fiber (MMF) is presented[32]. The sensing head is formed by insertion of a small section of MMF between a single-mode fiber (SMF) and the TFBG. The average reflective power in the cladding modes decreases with the increase of curvature. The measurement range of the curvature from 0 to 2.5m^{-1} with a measurement sensitivity of -802.4 nW/m^{-1} is achieved. The proposed sensor is also proved as temperature independent from the experimental investigation.

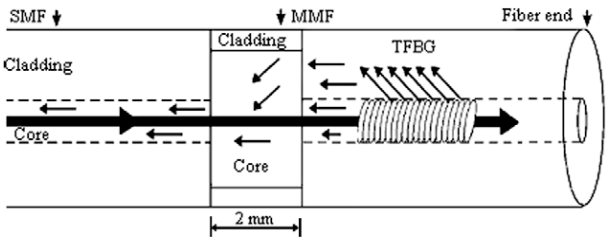

Fig. 14. Schematic diagram and principle of operation.

The proposed fiber bending sensor is shown in Fig.14. A section of 2mm MMF is spliced between the SMF and the TFBG. The MMF used in our experiment has a core diameter of 105μm. The TFBG had been manufactured by using a hydrogen-loaded SMF which was exposed on a frequency-doubled argon laser emitting at 244nm through a 1066nm uniform phase mask. The tilt angle was set to 5° and the length of the TFBG was 2cm.

The reflection spectra of the fiber bending sensor with an increasing curvature are shown in Fig.15. It can be seen that bending leads to attenuation in average cladding modes power but there is no apparent change in the Bragg reflection peak power, and its spectrum shape is well-maintained. Changing the curvature from 0 to 20m^{-1} resulted in more than 15-dB reduction of the average cladding modes power. When the bending effect was moved away from the sensor, the reflection spectrum returned to its initial state, showing that it had good stability and repeatability.

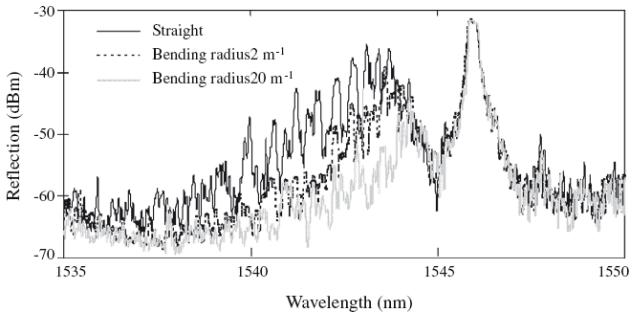

Fig.15. Spectrum response of cladding modes and Bragg mode resonances vs. curvature

4.1.6 Transverse Loading Sensors

A TFBG with a tilted structure at 81° was fabricated and the properties under transverse load applied to the equivalent fast and slow axes were studied[33]. The transverse loading experiment was implemented by first laying the 81°-TFBG fiber with the grating length of 12mm and a dummy fiber of the same type between two flat-surface aluminium plates, and then gradually increasing the load on the top of the plate with a loading length of 32mm. The schematic of the experiment is shown in Fig.16. The light from a broadband source (BBS) was launched into one end of the grating fiber and the output was monitored from the other end by an optical spectrum analyser (OSA). A linear polarizer and a polarization controller were inserted between the BBS and the TFBG to change the polarization state of the probing light. Before the transverse load was applied, we set the polarization state to fully excite the P1 mode by adjusting the polarization controller.

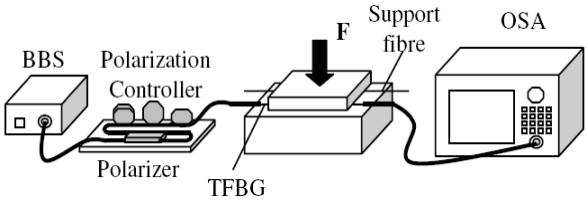

Fig.16. Schematic diagram of the transverse loading experiment system.

Fig.17 plots the normalized transmission losses against applied load for both peaks in linear scale. We can see from the figure that for the loading range from 3 to 31kg·m^{-1}, the transmission loss changes for P1 and P2 peaks are almost linear.

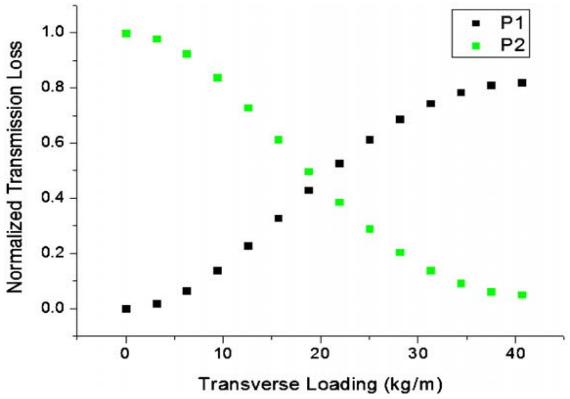

Fig. 17. Normalized transmission losses of the two orthogonal polarization modes plotted in linear scale with increasing load.

4.1.7 Displacement Sensors

Fig.18(*a*) shows the proposed sensing device[34]. It is made of highly elastic steel and its structure can be functionally divided into three parts: the sensing beam (top), the arc beam (vertical on the left) and the base. Displacement is vertically applied at the end of the sensing beam and the whole beam is supported by its base. A TFBG is axially pasted onto the outer surface of the arc beam with its central position parallel to the center of the semicircular hole.

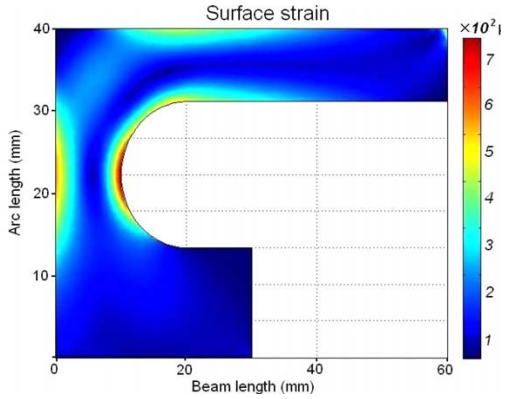

(a)

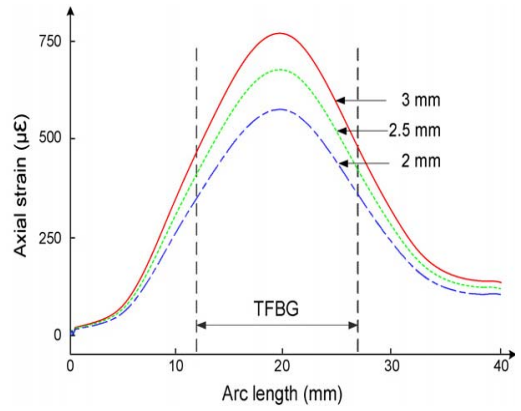

(b)

Fig.18 Sensing Structure and the finite element analysis of BCB under side-applied micro-displacement. (a) surface strain distribution (in color online) and (b) axial strain distribution along the outer surface of the side arc beam (three curves correspond to different displacements of the free end of the top sensing beam).

When displacement is vertically applied at the end of the sensing beam, the outer surface of the arc beam presents a non-uniform elongation and accordingly induces the same strain on the grating. Based on the finite element method, the displacement of the top sensing beam under side-applied displacement and the surface strain of the whole beam are analyzed, as shown in Fig.18(*a*). The corresponding strain profiles along the outer surface of the arc beam are evaluated when different displacements are applied, as shown in Fig. 18(b). Within the grating coverage (double dash lines marked in Fig.18(b)), a similar Gaussian strain profile has been achieved and the strain value is proportionally increased with the displacements applied.

The main new phenomenon that is peculiar to TFBG (relative to a straight FBG) is that the non-uniform spatial elongation (or compression) of the grating pitch also increases (or decreases) the internal tilt angle of the grating planes (originally 4°) with a similar distribution, as shown in Fig. 19. Within the grating coverage, there exists a quasi-Gaussian strain-gradient distribution, with a maximum at the central position and a smooth decrease at both ends. Under such a strain gradient distribution, the axial elongation of each grating pitch varies from its maximum at the grating center to its minimum at both ends. Also, along the fiber cross-section the spacing of the grating planes varies in an opposing trend, with its minimum at the grating center. With such a fiber shaping, the internal tilt angles of the grating planes have been modulated strongly at the grating center but change slightly at both ends. As a result, the phase matching condition for each value of the pitch is partly disrupted due to the non-uniform tilt plane modulation and to the stress-induced refractive index variation changes along the fiber cross-section. It was shown in [35,36] that bending leads to compressive and tensile strains on either side of the fiber axis (where the core is) and to a displacement of the mode field away from the core. Consequently, the mode coupling between the fiber core and the cladding weakens dramatically. Therefore, both the self coupling of the Bragg core mode and the core-to-cladding coupling of the ghost mode (which corresponds to a group of strongly coupled low-order cladding modes that interact much with the fiber core and are especially sensitive to bending) reduce with the displacement of the top beam. Consequently, when the displacement increases, a dramatically weakened ghost resonance results as shown in Fig.20.

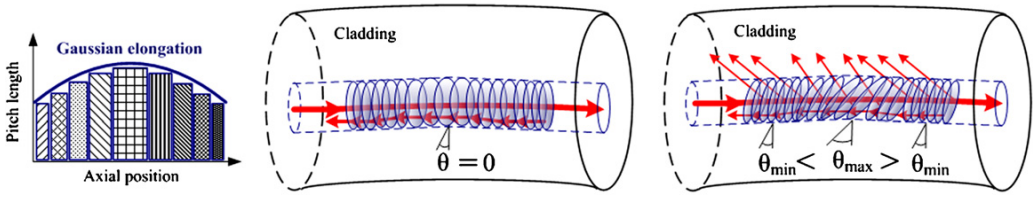

Fig.19 Comparison of straight FBG and TFBG under Gaussian elongation axial strain and the corresponding modulation of the internal pitch and tilt angle.

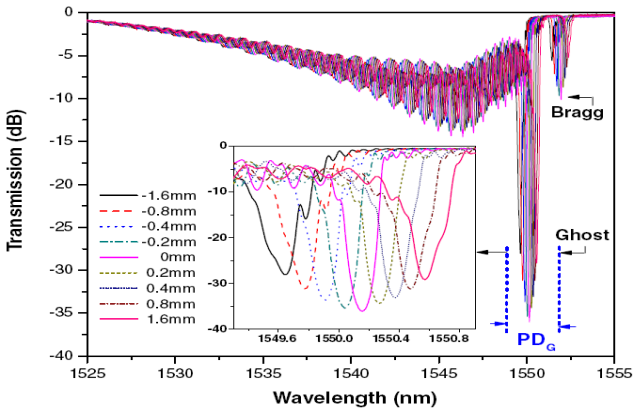

Fig.20 Transmission spectra of TFBG versus displacement at a fixed temperature of 20℃.

Fig. 21 shows the proposed sensing system. One centimeter long TFBG with an internal tilt angle of 4° is inscribed in hydrogen-loaded Corning SMF-28 fibers using a pulsed ArF excimer laser and the phase mask technique. After launching light from an erbium ASE broadband source (BBS) into the sensing fiber, the transmitted power of the sensing TFBG is filtered by a narrow band-pass filter (BF) within a concerned band and is then monitored by a PIN photodiode (PDG). Here, we use the optical spectrum analysis as a bandpass filter, measuring the total power in a 2nm wavelength interval (centered on the ghost resonance), as a function of displacement.

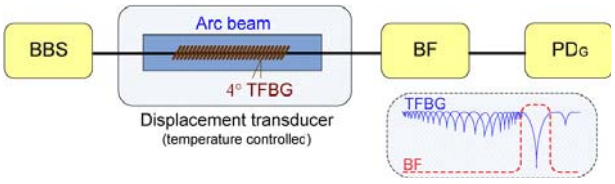

Fig.21 Schematic diagram of the displacement sensing system.

4.1.8 Measuring Modal Power Distribution

Modal power distribution (MPD) is an important feature of multimode fibers and multimode fiber devices. Chun Yang et al. (2005) proposed a novel MPD measuring method using Tilted fiber Bragg gratings[37].

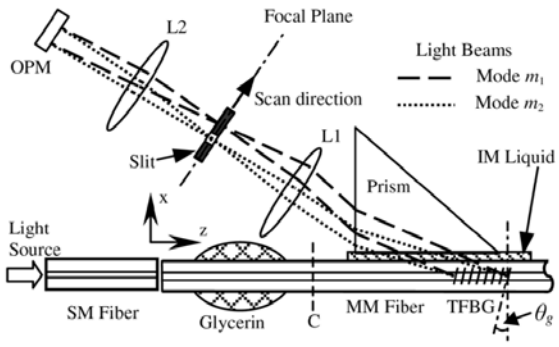

Fig. 22. System schematic of MPD measurement (L1, L2: Lenses; OPM: Optical power meter; IM: Index matching.)

As shown in Fig. 22, a multimode fiber is excited by a standard single-mode fiber with excitation condition adjustable. Glycerin was applied onto the fiber surface to remove the cladding modes of the MMF. The guided modes are coupled into the radiation modes through a TFBG imprinted in the same MMF, and refracted out of the fiber cladding through a prism and index matching liquid. A lens focuses the radiated light beams at different radiation angles on its focal plane, where a scanning slit is used to select and deliver part of the power from one of the radiation light beams to a power meter through another lens. The the m th guided power and the total light power can be calculated from radiation power which can be read out from the power meter directly.

Conventional MPD measurement methods based on the near- and/or far-field techniques require preliminary knowledge of refractive index profile of the fibers[38]. This TFBG based method MPD can be obtained by simply measuring the powers of radiation modes. The system is simple, compact and low cost. It is now successfully experimented with a few-mode fiber[4].

4.2 Novel optical devices and other applications

4.2.1 Wideband Gain Flattened Fiber Amplifier

Erbium doped fiber amplifiers (EDFAs) have been demonstrated with gains in excess of 50dB. However, one problem with the EDFA is its non-uniform gain spectrum which limits the bandwidth over which a constant gain can he achieved. R. Kashyap et al. (1993) successfully overcame the limitation by applying tilted fiber Bragg gratings in EDFAs[1].

Tilted fiber gratings can couple the guided mode to the radiation field. R. Kashyap et al. utilized the wavelength selective loss of titled fiber gratings and demonstrated a very flat amplified spontaneous emission (ASE) spectrum over a wide bandwidth in an erbium fiber amplifier. A 3mm long gratings with an angle θ to the normal to the axis of the fiber is formed on a Ge doped fiber, and then jointed with a 3m long erbium doped fiber. The guided mode will be coupled to the radiation field if the titled angle θ satisfy certain condition[1]. Curve (i) and (ii) in Fig.23 demonstrates that the ASE spectra of a 3m long erbium doped fiber amplifier when pumped with 15 mW of pump power at 980nm from a diode laser without and with tilted fiber Bragg gratings, respectively. With TFBG, we can see the light power near the peek has been flattened within ± 0.5 dB over the central 35nm[1].

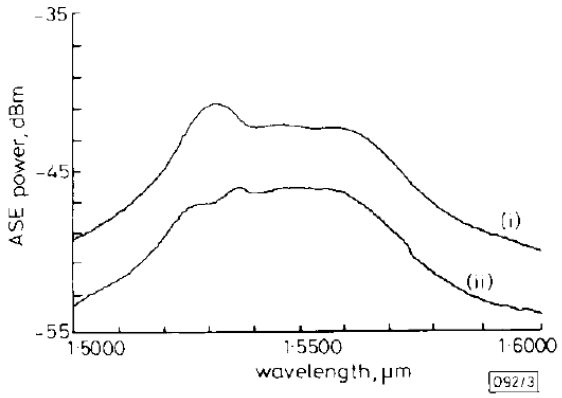

Fig.23 ASE spectra of erbium doped fiber[1] (i) Without tilted fiber Bragg gratings, (ii) With tilted fiber Bragg gratings.

This gain-flatten approach of EDFA is simpler in fabrication and easier to control the attenuation rate than other techniques, such as using pure $A1_2O_3$ core erbium doped fibers[26] or using phase gratings[27-29]. Compared with long period gratings (LPG) which can also be used as gain flattening filters for optical amplifiers, TFBGs have a number of advantages for use in devices, including low temperature sensitivity, the absence of sensitivity to bends and to the materials used for the cladding. The only drawback of the tilted fiber Bragg gratings is the back reflection, which can, however, be removed by careful choice of tilt angle.

4.2.2 Narrow-band optical fiber filters

TFBG can enable otherwise unallowed coupling between discrete bound modes of fiber such as the coupling between the LP01 mode and the LP11 mode. Based on this characteristic, TFBG can be practically useful in cases where large radiation or other bound mode coupling is desired but Bragg reflection is undesirable.[39]

This property can be used to investigate narrow-band optical fiber filters or Add-drop Multiplexer.

In 1998, Charles W. Haggans et al. utilize this property of TFBG in demonstrating a low-reflection channel-block bandpass filter with <-30 dB back-reflection at the peak rejection wavelength.

In this filter, TFBG couple light from the core of an optical fiber to the cladding at discrete wavelengths below the Bragg wavelength. These discrete couplings produce narrow attenuation bands in the transmitted spectrum. At an optimized tilt angle, power is efficiently coupled from the forward propagating LP01 mode to the counter-propagating LP11 hybrid mode. Since the LP11 hybrid mode is lossy, this power is lost from the fiber core over distance, giving narrow-band filtering with negligible back-reflection.

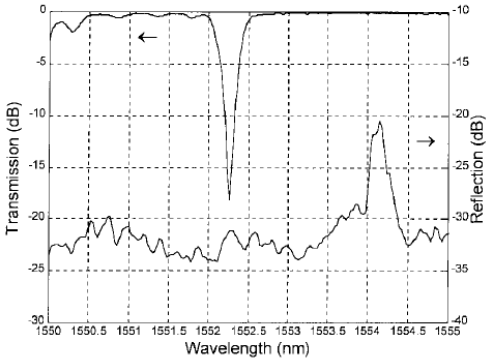

Fig.24. Transmission and reflection spectra for DIC fiber for in fiber fringe tilt of θ= 4.0.

Fig.24 is a plot of the transmission and reflection spectra for a grating with 4°. On this plot, the transmission minimum due to LP01 –LP01 coupling at 1554 nm is not distinguishable. The 2nm passband between the higher order loss notches (1550.25 nm) and the peak loss notch (1552.25 nm) allows for the application of this device in some bandpass filter applications. The reflection spectrum in Fig.24 demonstrates that reflection due to LP01 –LP01 coupling (1554 nm) is <-20 dB. However, reflection in the rejection band is <-30 dB.

Through the extension of the grating into the cladding region, which giving increased overlap of certain LP1m modes with the LP01 core mode, Charles achieved strong LP01 -LP1m coupling. The lossy nature of the LP1m cladding modes also gives negligible back-reflection for the appropriate tilt angle.

4.2.3 Add-drop Multiplexer

Tilted fiber Bragg grating can enable coupling between the LP01 mode and the LP11 mode, thus can be used to convert modes in an add-drop wavelength-division multiplexer.

Fig.25 shows the schematic of a novel allfiber add–drop multiplexer using a tilted Bragg grating written on a

two-mode fiber and a mode-selective coupler. [6]

The operating principle of the titled fiber Bragg grating add-drop multiplexer is as follows. When wavelength-multiplexed optical signals enter the SMF of the first MSC through the input port, the MSC couples all the light in the input SMF into the LP11 mode in the TMF. Then the tilted FBG reflects a particular wavelength channel corresponding to its resonant wavelength. At the same time, because of the tilt in the grating, the reflected light changes its mode from the LP11 mode to the LP01 mode. The reflected light then passes through the MSC without coupling and comes out of the device at the drop port. The other wavelength channels transmit through the FBG without the mode change and are directed to the output port by the second MSC. In the case of the "add" operation, the added signal in the LP01 mode is reflected and converted to the LP11 mode by the tilted FBG and then it is again directed to the output port.

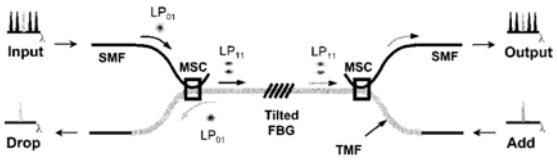

Fig.25 Schematic of add–drop multiplexer. (SMF: single-mode fiber; TMF: two-mode fiber; FBG: fiber Bragg grating; MSC: mode-selective coupler)[6]

Compared to integrated-optic or hybrid components, TFBG based add-drop multiplexer has following advantages. It is all fiber, low insertion loss and low cost. Besides, it has excellent and controllable spectral shapes as well.

4.2.4 In-fiber Polarimeters

Tilted fiber gratings can be functioned as highly polarization sensitive taps to couple light, which is linearly polarized along the grating tilt axis, out of the core mode. Thus, a number of in-fiber polarimeters based on TFBG is designed according to this characteristic[12-14, 40]. In order to determine the state of polarization, the polarimeter should contain at least two tilted gratings oriented to couple light out at different azimuthal angles around the fiber. However, gratings alone are not sufficient to differentiate right handed polarizations and left handed polarizations, since incident circular polarization would yield the same out-coupled light whether it is right or left handed circularly polarized. Therefore, another essential element in the polarimeter is the fiber waveplate which converts elliptically polarized light into differently oriented elliptical states depending on handedness. These states can then be discriminated by a subsequent tilted grating[40].

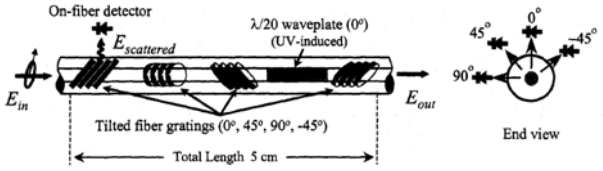

Fig. 26. Diagram of the TFBG based in-fiber polarimeter[14].

Fig.26 shows the schematic of the TFBG based in-fiber polarimeter which was proposed by P. S. Westbrook and T. A. Strasser[14]. Four tilted gratings which have a 45° tilted angle are imprinted at azimuthal angles of 0°, 45°, 90°, and –45°, and the waveplate is written between the last two gratings and oriented at 0°. Four on-fiber photon detectors are placed at each grating to monitor the scatter light. Stokes parameters can be obtained from the output of the four detectors.

Comparing with other fiber polarimeters, including designs using couplers[41, 42], and side-polished fibers[43], tilted fiber Bragg grating based polarimeters are more stable, compact, and easier to fabricate.

4.2.5 Polarization-dependent Loss Equalizer

PDL control and compensation is a subject of current research. Pavel Ivanoff D. C. Reyes, et al. (2003), fabricated highly tilted fiber gratings and demonstrated that the broad-band polarization-dependent loss (PDL) of the gratings may be tuned by twisting the fiber along the length of the grating [44].

45° tilted FBGs are known to have a broad-band polarization-dependent radiation mode loss. It is fixed to a clamp on one end and the other end attached to a rotating chuck as shown in Fig.27.

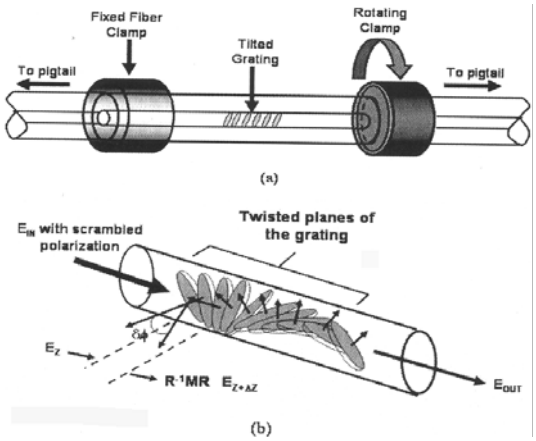

Fig. 27 (a) Schematic of the tilted fiber grating tunable PDL device, and (b) the grating planes that spiral when the fiber grating is twisted..

The range and sensitivity of the device PDL value is depending on the grating strength, grating length, and the azimuthal twist of the fiber grating. As the different parts of the grating are misaligned with respect to each other, PDL is reduced in the twisting process. By combining the twisted–tilted grating with a polarization controller, a PDL compensator can be formed. The primary advantage of this device is its small size, versatility, and compact in-fiber design.

5. Conclusions

As illustrated in the previous discussion , TFBG can be applied in real time spectrum monitor, strain, twist or chemical sensor, filter, refractometer, polarimeter, polarization-dependent loss equalizer and so on. These optical devices based on TFBG are always low-cost, compact and with low insertion loss.

The design of these devices mostly involves the tilted angle, which determine the mode coupling and the polarization dependence of the device, the grating index perturbation, controlling the coupling strength to the radiation mode due to the grating, the necessity of the index-matched prism or solution used to prevent strong coupling to fiber cladding modes. This offers sufficient degrees of design freedom to optimize the device for a variety of applications.

Recently, TFBG has been combined with other sensing mechanism, such as surface plasmon resonance[45], extending the foreground of this research field. Also, changing the shape and distribution of the grating planes may change the property of TFBG, which could be applied in new investigation of optical fiber sensors or devices.

Acknowledgements

Project 60704026 and 61074170 are supported by the National Science Foundation of China(NSFC). Project N090504002 and N100404006 are supported by the Fundamental Research Funds for the Central Universities.

References

[1] R. Kashyap, R. Wyatt, R. J. Campbell, Electronics Letters, **29**,154(1993).
[2] J. L. Wagener, T. A. Strasser, J. R. Pedrazzani, J. DeMarco, D. DiGiovanni, Fiber grating optical spectrum analyzer tap, Edinburgh, UK(1997).
[3] K. S. Feder, P. S. Westbrook, J. Ging, P. I. Reyes, G. E. Carver, IEEE Photonics Technology Letters, **15**, 933(2003).
[4] Y. Chun, W. Yong, X. Chang-Qing, IEEE Photonics Technology Letters, **17**, 2146(2005).
[5] J. M. Castro, D. F. Geraghty, B. R. West, S. Honkanen, Applied Optics, **43**, 6166(2004).
[6] H. S. Park, S. H. Yun, I. K. Hwang, S. B. Lee, B. Y. Kim, IEEE Photonics Technology Letters, **13**, 460(2001).
[7] C. Caucheteur, P. Megret, IEEE Photonics Technology Letters, **17**, 2703(2005).
[8] G. Laffon and P. Ferdinand,Measurement Science and Technology, **12**,765(2001).
[9] C.-F. Chan, G. Chen, A. Jafari, A. Laronche, D. J. Thomson, J. Albert, Applied Optics, **46**,1142(2007).
[10] K. Zhou, X. Chen, L. Zhang, I. Bennion, Optical chemsensors based on etched fibre Bragg gratings in D-shape and multimode fibres, Bruges, Belgium(2005).
[11] K. Zhou, X. Chen, L. Zhang, I. Bennion, Measurement Science and Technology, **17**, 1140(2006).
[12] J. Peupelmann, E. Krause, A. Bandemer, C. Schaffer, Electronics Letters, **38**, 1248(2002).
[13] A. Bouzid, M. A. G. Abushagur, A. El-Sabae, R. M. A. Azzam, Optics Communications, **118**, 329(1995).
[14] P. S. Westbrook, T. A. Strasser, Compact, in-line, all-fiber polarimeter using fiber gratings, Baltimore, MD, USA(2000).
[15] X. Chen, K. Zhou, L. Zhang, and I. Bennion, IEEE Photonics Technology Letters, **18**, 2596(2006).
[16] S. J. Mihailov, R. B. Walker, T. J. Stocki, D. C. Johnson, Electronics Letters, **37**, 284(2001).
[17] T. Erdogan, J. E. Sipe, Journal of the Optical Society of America A (Optics, Image Science and Vision), **13**, 296(1996).
[18] J. Grant, Y. Wang, and A. Sharma, Fabrication of a fiber-optic tilted Bragg grating filter in 40 nm range with a single phase mask, Quebec City, Canada(2002).
[19] M. C. P. Huy, G. Laffont, V. Dewynter, P. Ferdinand, L. Labonte, D. Pagnoux, P. Roy, W. Blanc, B. Dussardier, Optics Express, **14**, 10359(2006).
[20] T. Erdogan, Journal of Lightwave Technology, **15**,1277(1997).
[21] Meltz, G., Morey, W.W., Glenn, W.H.,In fiber Bragg grating tap, OFC ’90, 1990.
[22] Lee, M.K., Little, G.R., Opt. Eng.,**37**, 2687(1998).
[23] J. L. Arce-Diego, D. Pereda-Cubián, F. Fanjul-Vélez, Proc. of SPIE, 5840, 835(2005).
[24] G. Meltz, W. W. Morey, J. R. Dunphy, Fiber Bragg grating chemical sensor, Boston, MA, USA(1992).
[25] C. Jauregui, A. Quintela, J. M. Lopez-Higuera, Optics Letters, **29**,676(2004).
[26] C. Jauregui, Measurement Science and Technology, **15**, 1596(2004).
[27] K. Zhou, A. G. Simpson, X. Chen, L. Zhang, I. Bennion, IEEE Photonics Technology Letters, **16**, 1549(2004).
[28] A. G. Simpson, K. Zhou, L. Zhang, L. Everall, I. Bennion, Applied Optics, **43**, 33 (2004).
[29] C. Jauregui, A. Quintela, A. Cobo, M. A. Quintela, S. Diaz, J. M. Lopez-Higuera, Interrogation of interferometric sensors with a tilted fiber Bragg grating, Santander, Spain(2004).

[30] C. Caucheteur, F. Lhomme, K. Chah, M. Blondel, P. Megret, Use of tilted Bragg gratings to simultaneously measure sugar concentration and temperature during the production process of sugar, Bruges, Belgium(2005).
[31] K. Zhou, L. Zhang, X. Chen, I. Bennion, Journal of Lightwave Technology, **24**, 5087(2006).
[32] Y. X. Jin, C. C. Chan, X. Y.Dong, Y. F. Zhang, Optics Communications, **282**,3905(2009).
[33] R. Suo, X. Chen, K. Zhou, L. Zhang, I. Bennion , Measurement Science and Technology, **20**,034015(2009).
[34] T. Guo, C. Chen, J. Albert, Measurement Science and Technology, **20**,034007(2009).
[35] J. Dacles-Mariani, G. Rodrigue, J. Opt. Soc. Am. B, **23**, 1743(2006).
[36] R.T. Schermer, Opt. Express, **15**, 15674(2007).
[37] C. Yang, Y. Wang, C.-Q. Xu, IEEE Photonics Technology Letters, **17**, 2146(2005).
[38] D. Rittich, Journal of Lightwave Technology, **T-3**, 652(1985).
[39] Charles W. Haggans, Harmeet Singh, Wayne F. Varner, Yaowen Li, Mark Zippin, IEEE Photonics Technology Letters, **10**, 690(1998).
[40] P. S. Westbrook, T. A. Strasser, T. Erdogan, IEEE Photonics Technology Letters, **12**, 1352(2000).
[41] B. Scholl, T. Stein, A. Neues, K. Mertens, Optical Engineering, **34**, 1669(1995).
[42] S. M. Lee, W. Pan, C. Yang, Proceedings of SPIE, **2839**, 133(1996).
[43] B. Scholl, J. C. Rasmussen, H. J. Schmitt, Proceedings of SPIE, **2265**, 48(1994).
[44] Pavel Ivanoff D. C. Reyes, Paul S. Westbrook, IEEE Photonics Technology Letters, **15**, 828(2003).
[45] Yanina Y. Shevchenko, Anatoli Ianoul, Chengkun Chen, Jacques Albert, Proc. of SPIE, **6796**, 1Z1-12(2007).

*Corresponding author: zhaoyong@ise.neu.edu.cn